The rhizobial autotransporter determines the symbiotic nitrogen fixation activity of Lotus japonicus in a host-specific manner

doi: 10.1073/pnas.1913349117

The rhizobial autotransporter determines the symbiotic nitrogen fixation activity of *Lotus japonicus* in a host-specific manner

Yoshikazu Shimoda[a,1], Yuki Nishigaya[b], Hiroko Yamaya-Ito[a,c], Noritoshi Inagaki[b], Yosuke Umehara[a], Hideki Hirakawa[d], Shusei Sato[d,e], Toshimasa Yamazaki[b], and Makoto Hayashi[a,f]

[a]Institute of Agrobiological Sciences, National Agriculture and Food Research Organization, Tsukuba, Ibaraki 305-8634, Japan; [b]Advanced Analysis Center, National Agriculture and Food Research Organization, Tsukuba, Ibaraki 305-8602, Japan; [c]College of Bioresource Sciences, Nihon University, Fujisawa, Kanagawa 252-0880, Japan; [d]Department of Technology Development, Kazusa DNA Research Institute, Kisarazu, Chiba 292-0818, Japan; [e]Graduate School of Life Sciences, Tohoku University, Sendai, Miyagi 980-8577, Japan; and [f]Center for Sustainable Resource Science, RIKEN, Yokohama, Kanagawa 230-0045, Japan

Edited by Sharon R. Long, Stanford University, Stanford, CA, and approved December 12, 2019 (received for review August 4, 2019)

Leguminous plants establish endosymbiotic associations with rhizobia and form root nodules in which the rhizobia fix atmospheric nitrogen. The host plant and intracellular rhizobia strictly control this symbiotic nitrogen fixation. We recently reported a *Lotus japonicus* Fix$^-$ mutant, *apn1* (*aspartic peptidase nodule-induced 1*), that impairs symbiotic nitrogen fixation. APN1 encodes a nodule-specific aspartic peptidase involved in the Fix$^-$ phenotype in a rhizobial strain-specific manner. This host-strain specificity implies that some molecular interactions between host plant APN1 and rhizobial factors are required, although the biological function of APN1 in nodules and the mechanisms governing the interactions are unknown. To clarify how rhizobial factors are involved in strain-specific nitrogen fixation, we explored transposon mutants of *Mesorhizobium loti* strain TONO, which normally form Fix$^-$ nodules on *apn1* roots, and identified TONO mutants that formed Fix$^+$ nodules on *apn1*. The identified causal gene encodes an autotransporter, part of a protein secretion system of Gram-negative bacteria. Expression of the autotransporter gene in *M. loti* strain MAFF3030399, which normally forms Fix$^+$ nodules on *apn1* roots, resulted in Fix$^-$ nodules. The autotransporter of TONO functions to secrete a part of its own protein (a passenger domain) into extracellular spaces, and the recombinant APN1 protein cleaved the passenger protein in vitro. The *M. loti* autotransporter showed the activity to induce the genes involved in nodule senescence in a dose-dependent manner. Therefore, we conclude that the nodule-specific aspartic peptidase, APN1, suppresses negative effects of the rhizobial autotransporter in order to maintain effective symbiotic nitrogen fixation in root nodules.

legume–rhizobium symbiosis | nitrogen fixation | autotransporter

Leguminous plants establish endosymbiotic associations with nitrogen-fixing soil bacteria, called rhizobia, and form root nodules where resident rhizobia fix atmospheric nitrogen. The symbiotic nitrogen fixation by legumes is extremely important because it supplies a great amount of fixed nitrogen to ecosystems and contributes to crop production. The symbiotic association between legumes and rhizobia starts with mutual recognition of signal molecules secreted from both partners. In the rhizosphere, plant-derived flavonoids are perceived by the compatible rhizobia and induce the production of a lipochitooligosaccharide signal, called Nod factor (NF), by the rhizobia. NFs are perceived by the host legumes, resulting in the activation of subsequent symbiotic reactions that lead to rhizobial infection and nodule organogenesis. Forward genetic studies on two model legumes, *Lotus japonicus* and *Medicago truncatula*, have identified many components involved in the early steps of the root nodule symbiosis (reviewed in refs. 1–3). These include the perception of NFs by lysine-motif receptor kinases, followed by downstream calcium signaling via calcium calmodulin-dependent protein kinase and the activation of several transcription factors, such as CYCLOPS and NIN, involved in the transcriptional reprogramming of symbiotic cells (4–10).

Unlike the early steps of the nodulation process, the molecular mechanisms underlying the regulation of nitrogen fixation activities in root nodules are far less understood. However, studies of Fix$^-$ mutants of model legumes, which develop nodules with endosymbiotic rhizobia but are defective in nitrogen fixation, have revealed some biological processes required for symbiotic nitrogen fixation (reviewed in ref. 2). In *L. japonicus*, *SST1*, *SEN1*, *FEN1*, *IGN1*, and *SYP71* are necessary for nitrogen fixation activity and maturation of infected cells in nodules (11–15). A series of Fix$^-$ mutants, designated as *dnf1* to *dnf7* ("*defective in nitrogen fixation*"), that exhibit altered nitrogen fixation capacity, were identified in *M. truncatula*. Among the *dnf* mutants, *DNF1* and *DNF2* encode a subunit of the signal peptidase and phosphatidylinositol-specific phospholipase C, respectively (16, 17). In addition, the recent availability of genome sequences and accumulation of transcriptome data in model legumes also have enabled us to identify many nodule-specific genes presumed to be involved in symbiotic nitrogen fixation. For example, legumes belonging to the inverted-repeat lacking clade (IRLC), such as *Medicago* and *Pisum*, express hundreds of nodule-specific cysteine-rich (NCR) peptides in the infected cells (18), and the loss of the specific NCR peptides results in Fix$^-$ phenotypes (19, 20).

Significance

The root nodule symbiosis between legumes and nitrogen-fixing rhizobia is an important source of nitrogen in terrestrial ecosystems, and successful symbiotic nitrogen fixation (SNF) can substitute for the nitrogen fertilizers in agricultural lands. However, the efficiency of SNF varies greatly depending on the combination of legume and rhizobial genotypes, and the molecular mechanisms that determine the compatibility are largely unknown. By studying the *Lotus japonicus* symbiotic mutant, we discovered that the host plant nodule-specific peptidase and the protein secretion system of rhizobia (autotransporter) regulate the compatibility of SNF. Our findings reveal an aspect of the strategy of legumes to optimize SNF efficiency with specific rhizobial strains, which may contribute to the development of technologies to improve symbiotic performance.

Author contributions: Y.S., Y.N., H.Y.-I., Y.U., S.S., T.Y., and M.H. designed research; Y.S., Y.N., and N.I. performed research; Y.S., Y.N., N.I., H.H., and S.S. analyzed data; and Y.S., N.I., and M.H. wrote the paper.

The authors declare no competing interest.

This article is a PNAS Direct Submission.

Data deposition: Gene Expression Omnibus (GEO), accession number GSE129778.

[1]To whom correspondence may be addressed. Email: yshimoda@affrc.go.jp.

This article contains supporting information online at https://www.pnas.org/lookup/suppl/doi:10.1073/pnas.1913349117/-/DCSupplemental.

First published January 3, 2020.

Host legume proteins identified in Fix$^-$ mutants can be roughly categorized into three groups by their proposed functions in the nodule. The first category includes those involved in nodule-specific metabolism and transport from host cells to bacteroids, the intracellular form of rhizobia inside the nodule. For example, the nodule-specific sulfate transporter SST1 (11) mediates the supply of sulfate, and homocitrate synthase FEN1 (12) controls the supply of homocitrate, an essential component of the Fe-MO cofactor of the bacterial nitrogenase. *L. japonicus* SEN1 is proposed to act as an iron transporter in nodule infected cells (14). Reverse genetic approaches have also shown the presence of several transporters in nodules, such as those for citrate, dicarboxylate, and ammonium (21–24).

The second category includes proteins involved in bacteroid differentiation. In IRLC legumes, rhizobia inside the nodule cells undergo terminal differentiation into mature bacteroids, which is accompanied by cell enlargement, modification of membrane permeability, and polyploidy, and some NCR peptides are required in the process (25, 26). Despite the large size of the gene family, some of the NCR peptides have essential, nonredundant roles in controlling the differentiation of bacteroids and nitrogen fixation. NCR211 encoded by *DNF4* is required for the survival of differentiating bacteroids in nodules (20). NCR169 encoded by *DNF7* is essential for the complete differentiation of bacteroids (19). In addition to IRLC legumes, *Aeschynomene* spp. legumes belonging to the Dalbergioid clade use NCR-like peptides to impose terminal differentiation and the formation of spherical and/or elongated bacteroids on *Bradyrhizobium* spp. (27, 28). In non-IRLC legumes, such as *Lotus* and *Glycine* species, where rhizobium differentiation into bacteroids is not terminal, no NCR peptide-like genes have been found in their genomes (18), indicating that different mechanisms for bacteroid differentiation are expected.

The third category includes proteins that determine the compatibility between host legumes and rhizobial strains in symbiotic nitrogen fixation. Unique Fix$^-$ mutants and plant accessions were recently reported in *Lotus* and *Medicago*, which exhibited Fix$^-$ phenotypes in a manner specific to rhizobial strain or plant genotype. A series of studies on *M. truncatula* showed that two genes, *NFS1* and *NFS2*, restrict the nitrogen fixation of certain *Sinorhizobium* strains, A145 and Rm41 (29–31). *NFS1* and *NFS2* were shown to encode NCR peptides. When NFS1 and NFS2 were expressed, Rm41 bacteroids were eventually killed in planta and the nodule displayed Fix$^-$ phenotypes, indicating that these NCR peptides negatively control the bacteroid differentiation and survival in a rhizobial strain-specific manner. Although rhizobial targets for these NCR peptides remain unclear, these reports provided important evidence indicating that molecular interactions between host plants and rhizobia are involved in controlling the activity and compatibility of symbiotic nitrogen fixation.

We recently reported a novel Fix$^-$ mutant named *apn1* from *L. japonicus* that showed Fix$^-$ phenotypes in a rhizobial-strain-specific manner (32). Now we report *apn1* as a strain-specific Fix$^-$ mutant identified in *L. japonicus*. The *apn1* mutant showed typical Fix$^-$ phenotypes when inoculated with *Mesorhizobium loti* strain TONO (33, 34), but it formed effective nodules with nitrogen fixing activity when inoculated with *M. loti* strain MAFF303099 (35). APN1 encoded an aspartic peptidase expressed specifically in nodule infected cells (32). Although the function of APN1 in nodules remained unclear, the strain-specific Fix$^-$ phenotype of the *apn1* mutant strongly implied that some molecular interactions between the host plant and rhizobial factors were involved in the control of compatibility and nitrogen fixation activity of *L. japonicus*. Considering the absence of NCR-like peptides in non-IRLC legumes such as *Lotus*, it is thought that other mechanisms independent of NCR peptides regulate the nitrogen fixation activity by APN1 with specific rhizobial strains.

To gain deeper insight into the biological function of APN1 and to reveal the molecular mechanisms responsible for the strain-specific Fix$^-$ phenotype of *apn1*, here we explored rhizobial mutants that suppressed the Fix$^-$ phenotype of *apn1*. Based on large-scale mutant screening, we found the rhizobial autotransporter is a determinant of the nitrogen fixation activity of the *apn1* mutant. Our study revealed a molecular interaction between host plant nodule peptidase APN1 and the rhizobial autotransporter that controls rhizobial strain-specific nitrogen fixation activity.

Results

Comparison of Symbiotic Abilities between *M. loti* Strain MAFF303099 and TONO. *apn1* is a unique symbiotic mutant that shows a rhizobial strain-specific Fix$^-$ phenotype (32). On *apn1* roots, *M. loti* strain MAFF303099 forms pink mature nodules with nitrogen fixation activity, whereas strain TONO forms small dark brown or black nodules with low nitrogen fixation activity (Fig. 1*A*). Both strains form normal nodules on wild-type *L. japonicus* roots (32). Detailed observation of *apn1* Fix$^-$ nodules revealed that the degree of browning varies in individual nodules irrespective of size and developing stage of nodule (*SI Appendix*, Fig. S1 *A–D*), and the brown pigments did not always overlap the entire infected region (*SI Appendix*, Fig. S1 *E–G*). Even in the fully developed nodules, dark brown pigments were generally observed in the limited area of central infected region and, in some cases, in the nodule periphery layer (*SI Appendix*, Fig. S1 *E–G* and *N*). This implies that brown pigment is induced depending on a certain physiological status of host plant cells.

To compare the symbiotic abilities of the two strains in more detail, we analyzed infection and nodulation phenotypes in the wild type and the *apn1* mutant. Inoculation of GFP-labeled MAFF303099 and TONO with the *apn1* mutant showed that formation of infection threads and infection inside nodules were similar in both strains (Fig. 1 *B–E*). The lack of significant differences in the frequency of infection events (Fig. 1*F*) suggests that *apn1* is a mutant that shows symbiotic defects only in nitrogen fixation. At 4 wk after rhizobial inoculation, the number of nodules formed on the *apn1* roots was higher with inoculation of TONO than with MAFF303099 (Fig. 1*G*). Such an increase in the number of nodules has also been reported in other Fix$^-$ mutants (12, 17, 36), and this can be caused by deviation from the autoregulation of nodulation by the low nitrogen fixation activity of nodules. The competition assay with GFP- and GUS-labeled *M. loti* showed that, compared to strain TONO, MAFF303099 had a slightly higher competitiveness both in the wild type and the *apn1* mutant (Fig. 1*H*). Coinoculation of MAFF303099 and TONO to the *apn1* mutant did not complement the Fix$^-$ nodule phenotype of TONO (Fig. 1 *I–K*), indicating that symbiotic phenotypes of the *apn1* mutant are determined after rhizobial entry into the host plant cells.

Identification of *M. loti* Genes that Determine the Fix$^-$ Phenotype of *apn1*. The strain-specific Fix$^-$ phenotype of the *apn1* mutant implies that some molecular interactions between the host plant and rhizobial factors are involved in the compatibility of symbiotic nitrogen fixation. To identify rhizobial factors that determine the strain-specific Fix$^-$ phenotype of *apn1*, we first sequenced the whole genome of strain TONO and compared its gene composition with those of strain MAFF303099. The genome of TONO was ~8.4 Mb in size, and a total of 8,149 protein-coding genes were predicted (34). Comparison of predicted genes between MAFF303099 and TONO revealed that gene clusters involved in nodulation (*nod* genes), nitrogen fixation (*nif* and *fix* genes), the type III protein secretion system (T3SS), and exopolysaccharide production were highly conserved in their genome sequences and the order of genes (*SI Appendix*, Fig. S2), indicating that these genes were unlikely to be determinants of

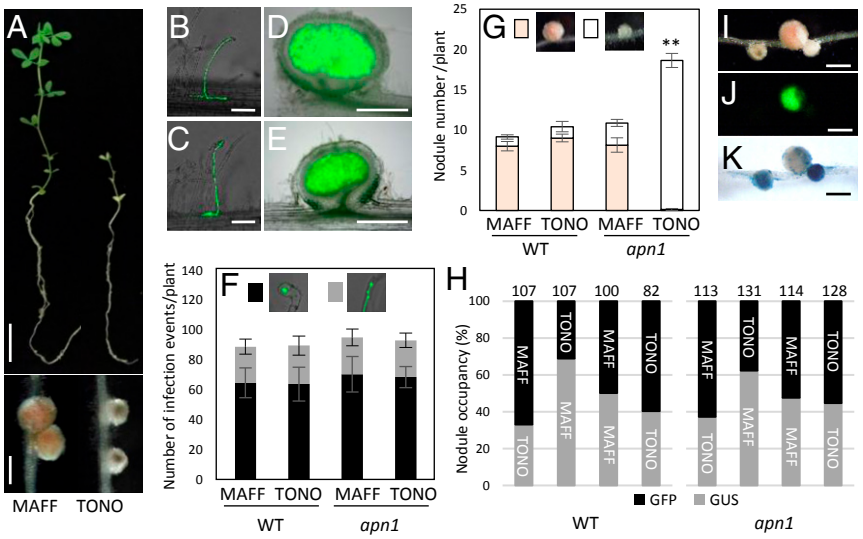

Fig. 1. Comparison of symbiotic properties between *M. loti* strain MAFF303099 and TONO. (*A*) Shoot growth (*Upper*) and nodule phenotype (*Lower*) of *apn1* mutant inoculated with *M. loti* strain MAFF303099 (MAFF, *Left*) and TONO (*Right*). Pictures were taken at 4 wk after *M. loti* inoculation. (Scale bars: *Upper*, 2 cm; *Lower*, 1 mm.) (*B–E*) Infection thread (*B* and *C*) and infection inside nodule (*D* and *E*) of *apn1* mutant visualized by GFP-expressing MAFF303099 (*B* and *D*) and TONO (*C* and *E*). Pictures are shown as a merged image of bright and fluorescence fields of GFP. (Scale bars: *B* and *C*, 100 μm; *D* and *E*, 500 μm.) (*F*) Frequency of infection events between MAFF303099 and TONO on wild-type (WT; MG-20 Miyakojima) and *apn1* mutant at 2 wk after *M. loti* inoculation. Bars represent the average number of microcolonies (black bars) and infection threads (gray bars) ± SEM ($n > 12$). No significant differences in the frequency of infection events were detected among the combinations of plant and rhizobia. (*G*) Nodule number formed on WT and *apn1* mutant inoculated with MAFF303099 and TONO. Number of mature pink nodules (pink bars) and Fix$^-$ nodules (white bars) were counted at 4 wk after inoculation. Bars represent the average number of each type of nodule ± SEM ($n > 8$). (*Insets*) Typical pink mature and Fix$^-$ nodules. Asterisk indicates statistical difference (**$P < 0.01$, Student's *t* test) in total and white nodule number between MAFF303099 and TONO. (*H*) Competition assays of MAFF30399 and TONO. Nodules were counted at 2 wk after inoculation with GFP- or GUS-labeled MAFF303099 or TONO. Numbers above the graph indicate the total number of nodules analyzed. (*I–K*) Nodule phenotype of the *apn1* mutant inoculated simultaneously with GFP-labeled MAFF30399 and GUS-labeled TONO. Bright-field (*I* and *K*) and fluorescence (*J*) images were captured. (Scale bars: 1 mm.)

the Fix$^-$ phenotype of *apn1*. This conclusion is also reasonable from the fact that both MAFF303099 and TONO can form nodules normally on wild-type *L. japonicus* (32). A genome-wide ortholog search between MAFF303099 and TONO identified genes present only in the TONO genome (34), but we could not specify any candidate genes because numerous genes were specific to each strain. Moreover, considering that some DNA sequence polymorphisms may affect the activity or function of genes, identification of candidate genes from the genome sequences alone is likely impossible.

As a second strategy, we constructed a transposon mutant library in strain TONO and explored mutants that could suppress the Fix$^-$ phenotype of *apn1*. TONO mutants were created using the Tn5 transposon by following the same procedures described by Shimoda et al. (37), and a total of 16,992 independent mutants were collected. When the mixtures of TONO mutants were inoculated with *apn1*, pink effective nodules were occasionally formed, along with many Fix$^-$ nodules, which resulted in promoted shoot growth (*SI Appendix*, Fig. S3). From the screening of 12,672 TONO mutants, we obtained a total of 242 pink effective nodules. To eliminate false positives, TONO mutants isolated from effective nodules were inoculated individually with *apn1* to confirm the formation of Fix$^+$ nodules, and transposon-disrupted genes were identified. From the series of mutant screening shown in *SI Appendix*, Table S1, we successfully identified one candidate TONO gene that determines the Fix$^-$ phenotype of the *apn1* mutant.

Characteristics of the Candidate Gene Product. The candidate gene identified from the mutant screening was MLTONO_0844 (34), which encoded a protein similar to a bacterial outer membrane autotransporter, also known as the type V protein secretion system. We named the identified TONO autotransporter gene DCA1 (Determinant of nitrogen fixation Compatibility of APN1). Domain search analyses revealed that a signal peptide (1 to 50 aa) and an autotransporter β-domain (IPR005546) were present at the N- and C-terminal ends of DCA1, respectively (Fig. 2*A*). Divergent glycine-rich motifs consisting of a unit of 44 to 53 aa were found 43 times between the signal peptide and the autotransporter β-domain (Fig. 2 *A* and *B* and *SI Appendix*, Fig. S4). Each glycine-rich motif was predicted to encode a β-sheet and a disordered coil structure (Fig. 2*B*). The glycine-rich repeat region that occupied a large part of DCA1 (>250 kDa) was predicted to form a β-helix structure, a typical trait of most autotransporter proteins (38, 39), and no known functional domains were predicted in the region. A BLAST search analysis found that the autotransporter proteins with similar long glycine-rich repeat regions existed not only in other rhizobia but also in other Gram-negative bacteria and cyanobacteria (Fig. 2*C*), but none of these proteins have had their biological functions proven so far. The BLAST search also revealed that several *Mesorhizobium* species, including strains MAFF303099 and R7A (40), possessed autotransporter proteins with high similarity to DCA1 of TONO (Fig. 2*C*).

From the large-scale mutant screening, we identified nine mutant alleles of *DCA1* (Fig. 2*A*, arrowheads, and *SI Appendix*, Fig. S5*A*). All mutant alleles were confirmed to contain transposon insertion inside *DCA1* (*SI Appendix*, Fig. S5 *B* and *C*) and formed pink mature nodules on *apn1* roots (*SI Appendix*, Fig. S5*D*), indicating that DCA1 was involved in the regulation of the nitrogen fixation activity of the *apn1* mutant. To further confirm whether DCA1 was responsible for the strain-specific Fix$^-$ phenotype of *apn1*, *DCA1* was introduced into strain MAFF303099, which formed nitrogen-fixing nodules on the *apn1* roots, and its symbiotic phenotype was analyzed. MAFF303099 harboring *DCA1* (MAFF_*DCA1*) formed small white Fix$^-$ nodules on *apn1* roots as

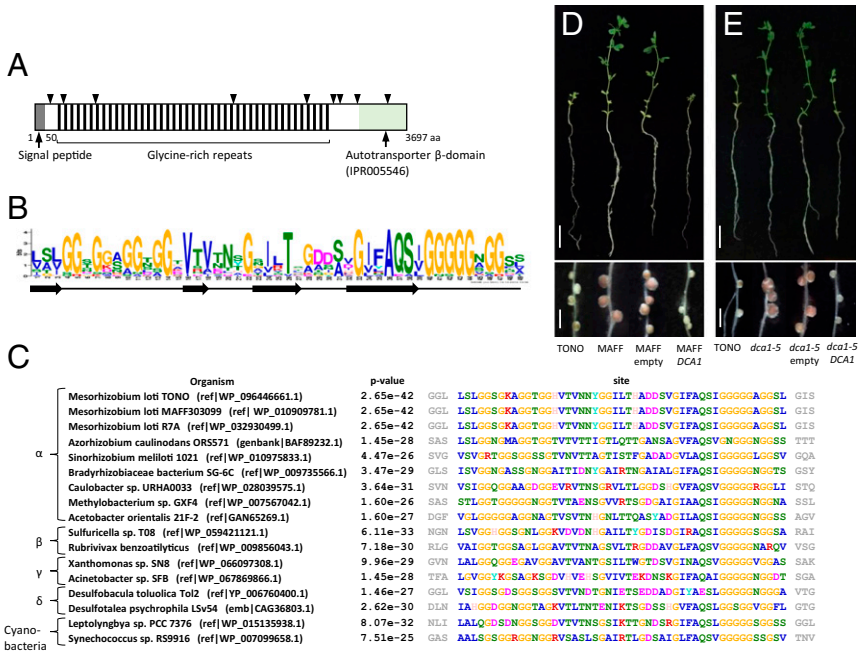

Fig. 2. Structure of *M. loti* autotransporter DCA1. (*A*) Domain structure of DCA1. Gray and pale green boxes at the N- and C-terminal ends indicate the signal peptide and autotransporter β-domain (IPR005546), respectively. Black lines indicate a unit of glycine-rich motif. Arrowheads above the image indicate the location of transposon insertion sites identified from mutant screening. (*B*) Amino acid composition probabilities in glycine-rich motifs of DCA1 homologs predicted by using the MEME tool (73). Arrows and line below the image indicate the secondary structure of β-strand and coiled region, as predicted by the PSI-PRED program (74). (*C*) Amino acid alignment of glycine-rich motifs found in representative DCA1 homologs of Gram-negative bacteria (α, β, γ, and δ proteobacteria) and cyanobacteria. (*D*) Shoot growth and nodulation phenotypes of *apn1* mutant inoculated with wild-type TONO, MAFF303099, and MAFF303099 harboring empty plasmid (MAFF_empty) or *DCA1* expressing plasmid (MAFF_*DCA1*). MAFF_*DCA1* formed small and white Fix$^-$ nodules, as did wild-type TONO. (*E*) Complementation test of *dca1* transposon mutant (*dca1-5*). *dca1-5* harboring *DCA1*-expressing plasmid (*dca1-5_DCA1*) complemented mutant phenotype and forms Fix$^-$ nodules, as did wild-type TONO. (Scale bars: *Upper*, 2 cm; *Lower*, 2 mm.)

in wild-type TONO, resulting in attenuated shoot growth (Fig. 2*D*). In contrast, the MAFF303099 control in which the empty vector was introduced (MAFF_empty) formed pink mature nodules as in wild-type MAFF303099 (Fig. 2*D*). In addition, *DCA1* successfully complemented its transposon mutant (*dca1-5*), resulting in the formation of Fix$^-$ nodules on *apn1* roots (Fig. 2*E*). These results clearly show that the identified autotransporter gene of TONO, *DCA1*, is a determinant of the strain-specific nitrogen fixation activity of the *apn1* mutant and that *DCA1* alone can completely alter the nitrogen fixation phenotype of MAFF303099.

We also analyzed other phenotypes of DCA1 transposon mutants, such as growth in culture media, motility, exopolysaccharide production, and nodulation ability on wild-type plants. However, no clear differences were found between wild-type TONO and the transposon mutants in all of the phonotypes tested (*SI Appendix*, Figs. S6 and S7), indicating that DCA1 was not involved in these biological processes.

DCA1 Has Activity to Secrete Protein to Extracellular Spaces. To reveal the structural features of DCA1, we conducted homology modeling. Since no appropriate PDB templates for the long glycine-rich repeat region of DCA1 (Fig. 2*A*) were available, we took advantage of the structure of the autotransporter β-domain (IPR005546) because some of its crystal structures had already been resolved. As a template for homology modeling, we used the crystal structure of Esterase A from *Pseudomonas aeruginosa* (EstA; PDB ID 3KVN) (41), which showed the highest BLAST score against the β-domain region of DCA1 (3330 to 3697 aa). The homology model by I-TASSER (42) revealed that the region of 3402 to 3697 aa formed a typical membrane barrel structure in which nearly polar and hydrophobic amino acid residues were located inside and outside of the barrel, respectively (Fig. 3*A* and *SI Appendix*, Fig. S8). The structural model also indicated that the region 3330 to 3402 aa formed an α-helix structure that passed through the barrel, and the N-terminal part from 3370 aa was located outside of the barrel.

Autotransporters have been reported to cleave a part of their own protein (the passenger domain) and to transport it to outside of the cell through the outer membrane-embedded barrel (43). To clarify whether DCA1 had the ability to transport protein to extracellular spaces, we first tried to identify the cleavage site of the DCA1 passenger domain. Because we expected that a sufficient amount of secreted proteins could not be obtained from rhizobia, we employed an IPTG-inducible protein expression system in *Escherichia coli.* Based on the homology model of DCA1, the protein region that was predicted to be located outside the barrel (N-terminal part from 3370 aa; Fig. 3*A*) was fused to the OmpA signal peptide of *E. coli* (MKKTAIAIAVALAGFATVAQA) (44), which allows periplasmic targeting, and three repeats of the myc epitope tag were inserted after OmpA (OmpA_myc_3252-3697; *SI Appendix*, Fig. S9*A*). The fusion fragment was cloned into the cold-inducible vector pColdI, and the protein was expressed in *E. coli* cells. After purification with myc tag (*SI Appendix*, Fig. S9*B*), a secreted protein fragment that could be seen with Coomassie Brilliant Blue staining was analyzed by mass spectrometry to determine the cleavage sites of DCA1. From the analysis, we successfully identified the cleavage sites of the DCA1 passenger domain at 3262 to 3265 aa (*SI Appendix*, Fig. S9 *C* and *D*).

To confirm the secretion of DCA1 passenger domain in *M. loti* cells, we next cloned the myc epitope tag-fused DCA1 into the pDG77 vector (45). As with *E. coli*, the myc epitope tag was placed after the signal peptide of DCA1 (1 to 50 aa) (Fig. 3*B*), and the resultant constructs were introduced into strain MAFF303099. We

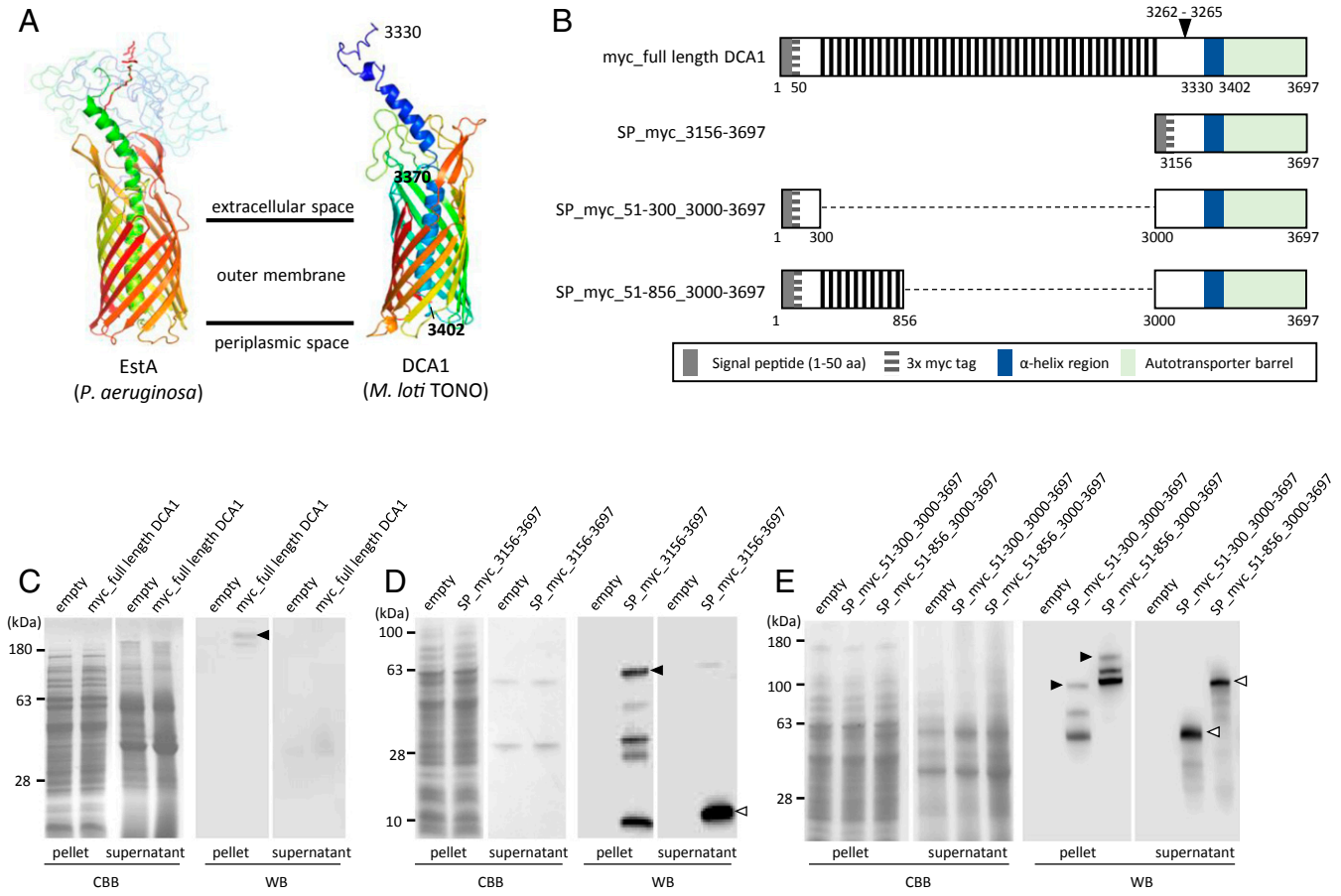

Fig. 3. Structure and protein secretion activity of DCA1. (*A*) Structure of the β-barrel region of DCA1, as predicted by homology modeling with the *P. aeruginosa* EstA protein as a modeling template. Structural models are colored by a gradient from blue at the N terminus to red at the C terminus. Localization of extracellular space, outer membrane, and periplasmic space is indicated according to the structure of EstA (41). Numbers on the model indicate the positions of amino acids. (*B*) Schematic illustrations of full-length and truncated DCA1 constructs used for the experiments in *C*–*E*. A black arrowhead indicates a cleavage site suggested in *SI Appendix*, Fig. S9. (*C* and *D*) Analysis of self-cleavage and secretion activity of full-length (*C*) and truncated DCA1 (*D*). CBB and WB indicate the images of Coomassie Brilliant Blue staining and Western blotting with anti-myc antibody, respectively. A black arrowhead in *C* is the signal of myc full-length DCA1 in cultured cell pellet. Black and white arrowheads in *D* indicate the signal of full-length SP_myc_3156-3697 in cultured cell pellet and secreted fragment in culture supernatant, respectively. (*E*) Determination of N-terminal secreted region of DCA1. Black arrowheads in pellet samples indicate the signals corresponding to the size of full-length SP_myc_51-300_3000-3697 and SP_myc_51-856_3000-3697. White arrowheads indicate the secreted fragments in culture supernatant. Western blotting was carried out against total proteins of cultured cell pellet and supernatant proteins precipitated by trichloroacetic acid.

first tried to confirm the expression and secretion using full-length DCA1, but no Western blot signals other than nonspecific ones were observed in culture supernatant proteins, and only a pellet sample gave faint signals (Fig. 3*C*). This likely occurred because the massive size of full-length DCA1 caused a low expression level. We then created an N-terminal truncated DCA1 construct (SP_myc_3156-3697; Fig. 3*B*), which contained a longer N-terminal region than that used in *E. coli* to allow easier detection via Western blotting. Western blotting with an anti-myc tag antibody showed a signal for a cultured cell pellet at around 63 kDa, which corresponded to the size of the introduced construct (Fig. 3*D*, black arrowhead). In the culture supernatant proteins purified by the anti-myc beads, a Western blotting signal was detected at ∼10 kDa, and it was not seen in the empty vector control (Fig. 3*D*, white arrowhead). The detected signal was somewhat smaller than expected from the cleavage site determined in *E. coli*, suggesting that additional cleavages might have occurred in *M. loti*. Our results indicate that DCA1 can transport a part of its own protein to the extracellular space.

To examine where the N-terminal end of DCA1 passenger domain was secreted, we next created other truncated DCA1 constructs in which the entire or the central glycine-rich repeat region was removed. SP_myc_51-300_3000-3697 had no glycine-rich repeats, whereas SP_myc_51-856_3000-3697 contained 10 of them (Fig. 3*B*). Western blotting against the total protein from the cultured cell pellet and supernatant detected the signals in both constructs (Fig. 3*E*), indicating that up to the entire N-terminal region without the signal peptide was secreted into the extracellular space.

We also tested the functionality of several truncated DCA1 proteins. When MAFF303099 harboring several truncated DCA1 constructs was inoculated with the *apn1* mutant, Fix$^-$ nodules were formed only when full-length DCA1 was introduced (*SI Appendix*, Fig. S10). This result indicates that the glycine-rich repeats, as well as its length, are important for the functionality of DCA1. This idea is also supported by the fact that the glycine-rich repeats are conserved as a long region in DCA1 homologs of other bacteria (Fig. 2*C*).

Peptidase Activity of Host Plant APN1 Is Required for Its Function in Root Nodule Symbiosis. Sequence analysis predicted that APN1 encodes an aspartic peptidase belonging to the subfamily A1B,

which includes *Arabidopsis* CDR1 and Nodulin 41 of *Phaseolus vulgaris* (PvNod41) (32, 46, 47). To investigate whether APN1 had properties of aspartic peptidases, we created a recombinant APN1 protein fused to the maltose binding protein (MBP) tag in *E. coli*. Aspartic peptidases may exhibit proteolytic activity under acidic conditions in which they self-cleave their own protein to exert maximum activity as a mature form (48). When purified MBP-APN1 was incubated in solutions of different pH (3.0 to 6.5), self-cleavage was observed under acidic conditions (Fig. 4*A*). This self-cleavage was clearly inhibited by pepstatin, an inhibitor of aspartic peptidases (Fig. 4*B*), as well as by mutations in two catalytically active sites of APN1 (D114N and D320N; Fig. 4*C*). These results indicate that APN1 has properties characteristic of aspartic peptidases.

The in vitro peptidase activity of APN1 prompted us to examine whether the peptidase activity of APN1 was required for its function in root nodule symbiosis. We performed a complementation assay of the *apn1* mutant with wild type and APN1 with mutated catalytically active sites (D114N and D320N). When inoculated with *M. loti* TONO, pink effective nodules were observed on the roots complemented with wild-type APN1, whereas nodules remained small and white with mutated APN1 (D320N and D114N_D320N; Fig. 4*D*). In the case of APN1(D114N), more pink nodules were formed compared to APN1(D320N) and APN1(D114N_D320N). These results indicate that the protease activity is required for the symbiotic function of APN1, and the D320 active site residue contributes significantly to the in planta activity of APN1.

Our data clearly show the one-for-one relationship between host plant APN1 and DCA1 of symbiotic rhizobia, which function as a peptidase and as protein secretion machinery, respectively. To clarify whether APN1 functions to degrade DCA1 in vitro, we created two N-terminal parts of DCA1 proteins without the signal peptide (51 to 300 aa and 51 to 856 aa), which were shown to be secreted into the extracellular space (Fig. 3*E*). These DCA1 proteins were expressed as fusion proteins with the GST tag. When MBP-APN1 was incubated with these substrates (GST-DCA1 51 to 300 aa and 51 to 856 aa, respectively) at pH 5.0, both substrates were degraded, whereas GST alone was not (Fig. 4*E*). Degradation was clearly inhibited by the addition of pepstatin (Fig. 4*E*) and by mutations in the active site of APN1 (D114N_D320N; *SI Appendix*, Fig. S11). These results indicate that DCA1 is a substrate degraded by APN1.

Promoter Activity of the *M. loti* Autotransporter Gene in Root Nodules. The presence of orthologous autotransporter genes in both MAFF303099 and TONO raised the question of how these genes caused opposite nitrogen fixation phenotypes of the *apn1* mutant. We first hypothesized that some specific protein regions determine the activity of respective *M. loti* autotransporters. To test this, we carried out a domain swapping experiment between DCA1 of TONO and its orthologous gene of MAFF303099 (gene ID *mll0950*). Unfortunately, we could not determine the regions responsible for the strain-specific phenotype because all swapping constructs showed the same phenotypes as intact DCA1. However, during the course of the domain swapping experiments, we found that mll0950, like DCA1, could completely convert the Fix^+ phenotype of MAFF303099 to Fix^- when it was expressed by the *trp*-promoter of the pDG77 vector (45) (*SI Appendix*, Fig. S12). This result implies that the difference in the expression level of the respective autotransporter gene determines the nitrogen fixation phenotypes of *apn1*. Therefore, we analyzed the promoter activities of mll0950 and DCA1 in nodules. The promoter-GUS assay showed stronger activity of the DCA1 promoter compared to that of mll0950 in both wild-type and *apn1* nodules (Fig. 5*A*).

Transcriptome Analysis of the *apn1* Nodules. To identify the host plant genes that were differentially regulated depending on *M. loti* strains, an RNA-seq analysis was carried out in the nodules

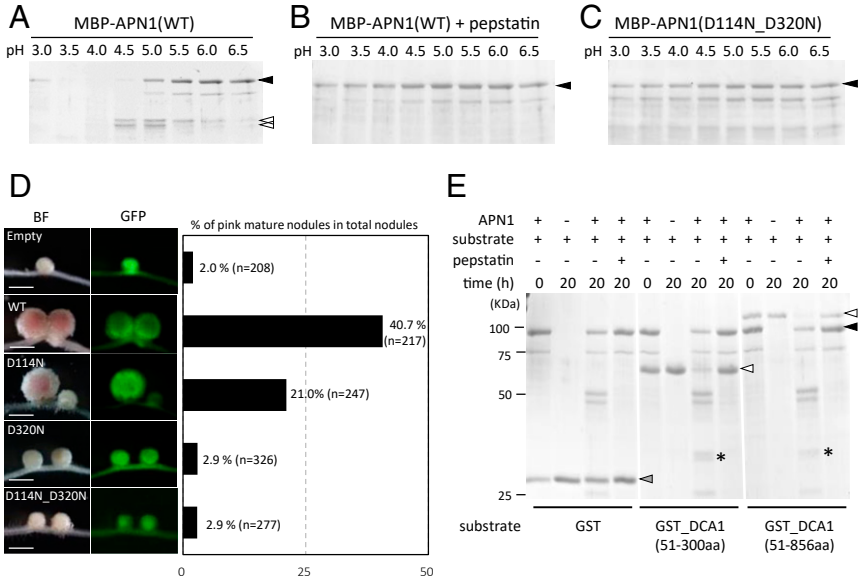

Fig. 4. Characterization of APN1 as an aspartic peptidase and requirement of peptidase activity for APN1 function in nodule symbiosis. (*A*–*C*) Self-cleavage activity of recombinant APN1 under different pH conditions (pH 3.0 to 6.5) (*A*). MBP-APN1 shows self-cleavage activity under acidic pH, and the activity is inhibited by the addition of 1 μM pepstatin (*B*) and mutations in two catalytic active sites of APN1 (D114N and D320N; *C*). Black and white arrowheads indicate MBP-APN1 and its cleaved products, respectively. (*D*) Complementation test of *apn1* mutant with wild-type (WT) APN1 and APN1 with the catalytically active site mutated (D114, D320N, and D114N_D320N). Images are representative nodules formed on transformed hairy root expressing GFP as a transformation marker. (Scale bars: 1 mm.) The accompanying graph shows the complementation activity of introduced APN1, analyzed by the percentage of mature pink nodules in total nodules formed on transgenic roots inoculated with TONO. n indicates the total number of nodules analyzed. (*E*) In vitro digestion of N-terminal DCA1 proteins by APN1. Black and white arrowheads indicate MBP-APN1 and two truncated DCA1 proteins (51 to 300 aa and 51 to 856 aa), respectively. Gray arrowhead indicates the GST. Asterisks indicate the cleaved products of DCA1 by APN1.

of the wild type (MG-20 Miyakojima) and *apn1* mutant formed by the inoculation with MAFF303099 or TONO. Differentially expressed genes specific to *apn1* Fix$^-$ nodules are listed in *SI Appendix*, Fig. S13 and Table S2. At 5 and 7 d after *M. loti* inoculation (dai), when no visible phenotypic differences of nodules were observed between MAFF303099 and TONO (*SI Appendix*, Fig. S13*A*), fewer genes were differentially expressed in *apn1* Fix$^-$ nodules than were common between Fix$^+$ and Fix$^-$ *apn1* nodules (*SI Appendix*, Fig. S14 and Table S3), indicating that only minor changes of gene expression might provoke nitrogen fixation deficiency in the *apn1* mutant. Among the specifically regulated genes in *apn1* Fix$^-$ nodules, the gene encoding cysteine protease (chr3.LjB03G07.10.r2.a) belonging to the senescence-associated gene 12 (SAG12) family (49) was significantly up-regulated at 7 dai (*SI Appendix*, Fig. S13*C* and Table S2). Orthologous cysteine protease genes of *M. truncatula* and soybean were reported to be induced in old or stress-treated nodules (50, 51). Real-time RT-PCR verified expression of the cysteine protease gene in the nodules formed by inoculation with MAFF303099 overexpressing *DCA1* (MAFF_*DCA1*) or with two DCA1 transposon mutants (*dca1-1* and *-5*). At 7 dai, chr3.LjB03G07.10.r2.a was clearly induced in nodules formed by inoculation with TONO, which was much higher in those inoculated with MAFF_*DCA1* as compared to those with wild-type MAFF303099 and two transposon mutants (Fig. 5*B*). Induction of the cysteine protease gene was more apparent in 10-dai nodules of TONO and MAFF_*DCA1*, and the latter was several tens of times higher than the former (Fig. 5*B*). *L. japonicus* has another cysteine protease gene cluster of the SAG12 family (chr3.CM0649.-270.r2.d, -280.r2.d, -300.r2.d, and -310.r2.d; *SI Appendix*, Fig. S15), and, in the RNA-seq analysis, these cysteine protease genes were not differentially expressed in *apn1* Fix$^-$ nodules. Consistent with the RNA-seq data, RT-PCR analysis showed that chr3.CM0649 genes were not induced in *apn1* nodules when analyzed with PCR primers that simultaneously amplify the chr3.CM0649 genes (Fig. 5*C*). However, these cysteine protease genes were significantly up-regulated in 10-dai Fix$^-$ nodules induced by MAFF_*DCA1* (Fig. 5*C*). Thus, our expression analyses show that, in the absence of functional APN1, DCA1 induces cysteine protease genes depending on its expression and activity.

M. loti strain TONO formed dark brown nodules on the root of *apn1* mutant (Fig. 1*A* and *SI Appendix*, Fig. S1) (32). In *M. truncatula*, such accumulations of brown pigment in nodules were associated with the induction of defense responses (17, 36, 52, 53). To clarify whether the defense responses were induced in *apn1* Fix$^-$ nodules, we examined the expression of some defense-related *Medicago* gene homologs in *L. japonicus*. Up to 10 dai, no significant induction of defense gene homologs was observed in TONO Fix$^-$ nodules compared to Fix$^+$ nodules induced by MAFF303099 (*SI Appendix*, Fig. S16). In the one exception, the gene encoding a vacuole processing enzyme (VPE; Lj5g3v0369970.1) showed a slight but significant increase in 10-dai Fix$^-$ nodules, which was enhanced by the overexpression of DCA1 (*SI Appendix*, Fig. S17).

Expression of Cysteine Protease and DCA1 Negatively Affect the Symbiotic Nitrogen Fixation. To clarify the role of the cysteine protease gene induced by DCA1 in nodule symbiosis, we examined the effects of overexpression of cysteine protease genes on nodule phenotypes. When cysteine protease genes, chr3.LjB03G07.10.r2.a

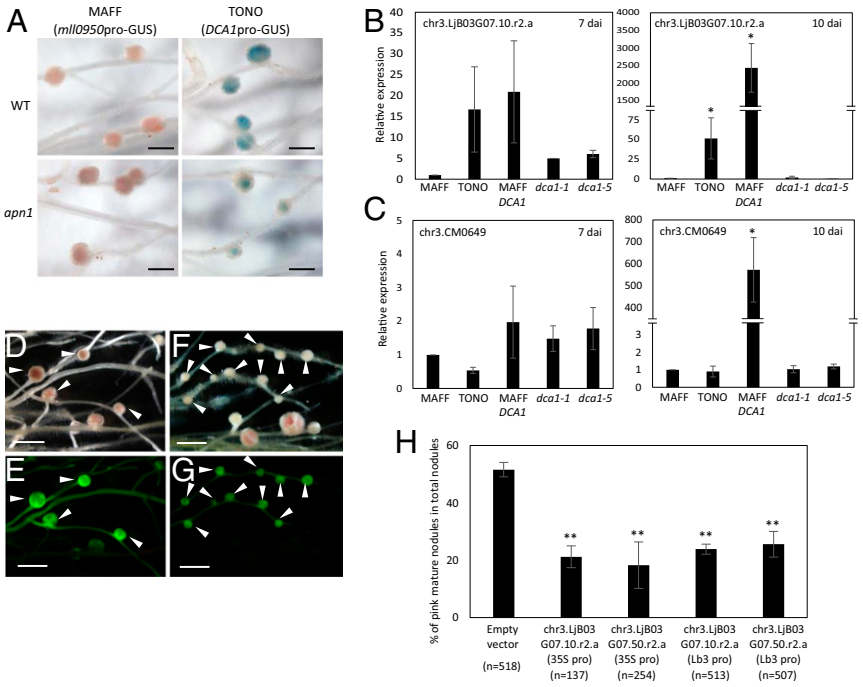

Fig. 5. Promoter activity of *M. loti* autotransporter and induction of cysteine protease genes by DCA1. (*A*) Promoter-GUS assay of DCA1 and mll0950 in nodules of wild-type (WT; MG-20 Miyakojima) and *apn1* mutant at 14 d after inoculation. (Scale bars: 1 mm.) (*B* and *C*) Expression of two groups of cysteine protease genes, chr3.LjB03G07.10.r2.a (*B*) and chr3.CM0649 (*C*), in *apn1* nodules at 7 and 10 d after *M. loti* inoculation (dai). Bars represent the mean values ± SEM of four independent experiments and are shown as relative expression to the level of MAFF nodules that is set to 1. All values were normalized against the expression of a reference gene, elongation factor 1 alfa. Asterisks indicate the significance of differences from MAFF nodule (*$P < 0.05$, Student's *t* test). (*D*–*G*) Representative images of nodules formed on hairy roots transformed with the empty vector (*D* and *E*) and with vector carrying construct overexpressing cysteine protease gene chr3.LjB03G07.10.r2.a (*F* and *G*). Arrowheads indicate the nodules formed on the transformed hairy roots. Pictures were taken under bright (*D* and *F*) and fluorescence field of GFP (*E* and *G*). (Scale bars: 2 mm.) (*H*) Percentage of mature pink nodules in total nodules formed on hairy roots transformed with cysteine protease genes. Bars represent the mean values ± SEM of three independent experiments. n indicates the total number of nodules analyzed. Asterisks indicate the significance of differences from empty vector (**$P < 0.01$, Student's *t* test).

and its paralogous gene (chr3.LjB03G07.50.r2.a; *SI Appendix*, Fig. S15), were expressed by CaMV 35S promoter or by the nodule-specific leghemoglobin (LjLb3) promoter, formation of effective nodules was significantly decreased compared to empty vector (Fig. 5 *D–H*). Thus, the cysteine proteases negatively affect nodule maturation, resulting in an increase of ineffective nodules. We also analyzed the effect of *DCA1* overexpression on nodule symbiosis. In the wild-type plant, MAFF303099 with *DCA1* overexpression (MAFF_*DCA1*) formed more immature nodules compared to wild-type MAFF303099 at 4 wk after inoculation (*SI Appendix*, Fig. S18*A*), leading to reduced shoot growth and nitrogen fixation activity (*SI Appendix*, Fig. S18 *B–D*). Because the expression of *DCA1* had no significant effects on the growth and nitrogen assimilation of plants (*SI Appendix*, Fig. S19), the reduction in the shoot growth of MAFF_*DCA1* inoculated wild type plants appears to be due to the reduced nitrogen fixation by DCA1 (*SI Appendix*, Fig. S18*D*). These phenotypes likely arose because APN1 could not completely suppress the effects of DCA1. In addition, wild-type MAFF303099 formed more immature nodules on *apn1* than wild-type roots, perhaps because weak but residual activity of the MAFF3033099 autotransporter appeared in the absence of functional APN1 (*SI Appendix*, Fig. S18*A*).

Discussion

The symbiotic nitrogen fixation in root nodules is strictly controlled by complex interactions between host legumes and intracellular rhizobia, and the activity greatly varies depending on the combination of both partners at species or genotypic levels. Strain-specific Fix$^-$ phenotypes have been described in many legumes, such as soybean, pea, and vetch (54–56), although responsible genes for the interaction have not been identified until recently. Studies on *M. truncatula* revealed the host secreted NCR peptides (encoded by *NFS1* and *NFS2*) were responsible for the strain-specific nitrogen fixation activity (29, 31), but the rhizobial targets of these peptides remained unclear. We recently identified *apn1* as the first *L. japonicus* Fix$^-$ mutant showing rhizobial strain-specific nitrogen fixation (32). Because no NCR-like peptides exist in non-IRLC legumes such as *Lotus* and *Glycine*, functional analysis of APN1 and identification of its molecular targets are expected to clarify novel regulatory mechanisms of the symbiotic compatibility that is independent of NCR peptides. By performing large-scale screening of *M. loti* mutants, here we identified the rhizobial autotransporter as a determinant of the strain-specific nitrogen fixation activity of *apn1*.

Autotransporter, also known as the type V secretion system, is one protein secretion system in Gram-negative bacteria. Autotransporters have multiple roles in biofilm formation, aggregation, and bacterial adhesion to or invasion of the host cells (43, 57, 58). Generally, an autotransporter consists of three functional domains: (*i*) the N-terminal signal peptide that mediates the translocation of the autotransporter into the periplasmic space through the SecYEG translocon, (*ii*) the central passenger domain, and (*iii*) the C-terminal β-domain that forms a β-barrel structure inside the outer membrane and allows translocation of the passenger domain to the bacterial cell surface (43, 58). As the name implies, an autotransporter secretes a part of its own protein (the passenger domain) as an effector protein, whereas, in other bacterial secretion systems, effector proteins and secretion machineries are encoded in distinct genes. Many varieties of passenger domains exist, and this variation confers the diverse functions of autotransporters. For example, the passenger domain of AIDA from animal and plant pathogenic bacteria, such as *E. coli* and *Agrobacterium tumefaciens*, plays a role in adherence to host cells. The bacterial pathogens *Haemophilus influenzae* and *Neisseria meningitidis* produce several proteases that degrade mammalian immunoglobulins by their autotransporters (43).

The autotransporter of *M. loti* (DCA1) that we identified here has a unique passenger domain that consists of extremely long glycine-rich repeats (>250 kDa). As with other autotransporters, DCA1 secretes its passenger domain into the extracellular space (Fig. 3*D*), and the entire glycine-rich region was found to be secreted (Fig. 3*E*). Homologous autotransporter proteins with similar long glycine-rich repeats exist in other bacteria, including rhizobia and cyanobacteria (Fig. 2*C*), but none of their biological functions have yet been revealed. This report shows the function of this type of autotransporter in a plant–microbe interaction. An autotransporter of *Azorhizobium caulinodans*, AoaA, was required for sustaining a high level of nitrogen fixation activity of stem nodules of *Sesbania rostrata*; a transposon mutant of AoaA exhibited reduced nitrogen fixation activity and was defective in exopolysaccharide production (59). Although AoaA (gene ID Azc_2635) structurally resembled DCA1, it was not a homolog of DCA1 because glycine-rich motifs were not conserved. Instead, Azc_3234 had similar glycine-rich motifs to DCA1 (Fig. 2*C*) and was therefore a homolog of DCA1. The functional difference between AoaA and DCA1 was also clear in our phenotypic characterization of the *dca1* mutants, which showed normal exopolysaccharide production and effective pink mature nodule formation on wild-type plants (*SI Appendix*, Figs. S6*D* and S7). Expression of DCA1 in MAFF303099 completely altered the nitrogen fixation phenotype of *apn1* nodule from Fix$^+$ to Fix$^-$ (Fig. 2*D*). In contrast, loss of function in DCA1 rescued the nitrogen fixation deficiency of *apn1* (*SI Appendix*, Fig. S5). This mode of action indicates that DCA1 is a key regulator of strain-specific nitrogen fixation activity.

The *apn1* mutant forms dark brown nodules by inoculation with *M. loti* strain TONO (Fig. 1) (32). Similar Fix$^-$ mutants that form brownish nodules have also been reported in *M. truncatula* (17, 36, 52, 53, 60). All causal genes of these *Medicago* mutants (*DNF2*, *RSD*, *SymCRK*, *Nad1*, and NPD1) express specifically in nodules but encode different types of proteins (DNF2, phosphatidylinositol phospholipase C-like protein; RSD, Transcription Factor; SymCRK, receptor-like kinase; Nad1, an uncharacterized protein with the transmembrane domain; NDP1, polycystin-1, lipoxygenase, a-toxin [PLAT] domain containing protein). Despite their types of proteins, the same defense-related proteins, such as PR10, chitinase, and nonrace-specific disease resistance 1 (NDR1), were induced in these mutant nodules, indicating that these genes control/suppress defense reactions that otherwise are triggered after bacterial release into nodule cells. Based on epistatic analysis, Berrabah et al. (61) proposed that DNF2 and symCRK/RSD are involved in distinct steps during bacteroid persistence. Although *APN1* of *L. japonicus* shared similar characteristics with these *Medicago* genes—namely, nodule-specific expression and dark brown nodule formation on the mutant—our gene expression analysis revealed that defense-related genes analyzed in *Medicago* Fix$^-$ nodules were not induced (*SI Appendix*, Fig. S16). In addition, enhanced autofluorescence indicative of phenolic compound accumulation (17, 53) was not observed on the dark brown pigments in the *apn1* nodules (*SI Appendix*, Fig. S1 *H–M*). These results indicate that similar defense-like reactions observed in *Medicago* mutants are not triggered in the *apn1* Fix$^-$ nodules, and APN1 is therefore thought to be involved in different symbiotic processes than those in which DNF2, RSD, SymCRK, and Nad1 are involved. Among the defense-related genes, only one gene encoding a VPE was induced by inoculation with TONO, and more strongly by MAFF303099 expressing DCA1 (*SI Appendix*, Fig. S17). VPEs belong to the C13 cysteine protease family resembling mammalian caspases and appear to be involved in the senescence process by contributing to the maturation or activation of other proteases (62). Genes encoding VPEs are strongly induced in old senesced nodules of soybean and *Medicago* (51, 63).

Formation of brownish nodules and induction of defense-related genes are not necessarily caused by nitrogen fixation

deficiency. Most rhizobial and host legume Fix$^-$ mutants do not form brownish nodules, and defense-like responses are not always associated with Fix$^-$ nodules (60, 61, 64, 65). This is also true of the *apn1* mutant. Dark brown nodule formation by the inoculation of TONO was not observed at all when the *M. loti* autotransporter gene (*DCA1* or *mll0950*) was overexpressed in MAFF303099 and TONO, even though all of the cases exhibited Fix$^-$ phenotype (*SI Appendix*, Fig. S12). In addition, overexpression of *DCA1* in MAFF303099 did not induce defense-related genes that were induced in the *Medicago* Nad1 mutant (*SI Appendix*, Fig. S16). Further analyses are necessary to clarify the relationships between the host defense responses and nitrogen fixation deficiency.

Although the precise function of the *M. loti* autotransporter in symbiotic nitrogen fixation is currently unknown, its genetic interaction with APN1 is apparent from the symbiotic phenotypes. Based on our results, we propose a functional model between APN1 and the *M. loti* autotransporter (*SI Appendix*, Fig. S20). Nitrogen fixation activity clearly depends on the presence of functional APN1 and the activity of the *M. loti* autotransporter. In wild-type nodules, the effector protein from the autotransporter is proposed to be degraded by APN1, resulting in suppression of the effect of the autotransporter. In contrast, the effect of the *M. loti* autotransporter on the nitrogen fixation becomes apparent in the *apn1* nodules where the effector protein is not degraded by APN1. Because strain MAFF303099 showed lower promoter activity of the autotransporter gene compared to strain TONO (Fig. 5*A*), effects of the autotransporter are not visible, whether in wild-type or *apn1* nodules. When the effector protein is not degraded by APN1, the presence of the effector protein eventually induces the expression of cysteine protease genes (Fig. 5*B*), leading to the suppression of nodule maturation and hence to the inhibition of symbiotic nitrogen fixation (Fig. 5 *D–H*). Involvement of cysteine proteases in symbiotic nitrogen fixation was also reported in *M. truncatula*, and expression of cysteine protease (*MtCP6*) and VPE (*MtVPE*) promoted nodule senescence (63). The relationship between APN1 and the *M. loti* autotransporter was also supported by our time-course phenotypic characterization with the DCA1 overexpressor (*SI Appendix*, Fig. S18). These results indicate that the qualitative and quantitative balances between APN1 and the autotransporter control the symbiotic nitrogen fixation activity.

Although our model explains the functional relationships between APN1 and DCA1, questions remain regarding where these proteins are targeted and where their protein interaction occurs in nodules. Despite several attempts, we have not obtained reliable results to answer these questions. Because the *APN1* gene is exclusively expressed in nodule infected cells (32) and the ortholog of *APN1* in soybean (Glyma15g260700) was shown to exist in the peribacteroid space by proteomic analysis (66), APN1 is assumed to be localized in the peribacteroid space. In addition, the peribacteroid space is known to be in an acidic state (67), the condition in which APN1 is active. Considering that the passenger domain of DCA1 is secreted extracellularly, the interaction between APN1 and DCA1 most likely takes place in the peribacteroid space. Although we showed that APN1 degraded N-terminal parts of the DCA1 passenger domain in vitro (Fig. 4*E*), it also remains unknown whether, in the *apn1* mutant, the DCA1 passenger domain remains in the peribacteroid space or moves through the peribacteroid membrane to exert its function. Detection of the intact DCA1 passenger domain in the *apn1* mutant is required to understand the mode of action of DCA1 on symbiotic nitrogen fixation.

The ecological significance of the DCA1-type autotransporter in rhizobia remains unclear. However, considering its ability to secrete the effector protein into extracellular spaces, this type of autotransporter is presumed to have roles in responses or adaptation to the surrounding environment, such as cell-to-cell communication with the same or different rhizobial species, as well as interactions with other organisms, including plants and other soil microbes. Our competition assay showed a comparable infection activity between MAFF303099 and TONO (Fig. 1*H*), indicating that expression of autotransporter does not affect the competition under these artificial conditions. However, the autotransporter may be involved in survival and/or competition in the natural rhizosphere where many plants and microorganisms exist.

Expression of *M. loti* autotransporter has a negative effect on nitrogen fixation depending on the presence of host plant APN1. Such rhizobial factors that negatively affect nodule symbiosis have been reported. For example, the Type III secretion system of several rhizobial species has negative effects on nodulation depending on plant species (summarized in ref. 68) and genotypes, such as *Rj* genes in soybean (69, 70). In *Sinorhizobium meliloti*, host-range restriction peptidase (hrrP) encoded by naturally occurring plasmid (pHRs) has a negative impact on nitrogen fixation depending on the host plant genotype (71). HrrP was proposed to play a role in the adaptation of sensitivity against variation of host-derived NCR peptides, and expression of HrrP promoted the proliferation of rhizobia in nodules (71). These reports strongly imply that, during evolution, legumes and rhizobia have acquired a multistep signal exchange mechanism for the selection of favorable symbiotic partners to initiate and maintain effective nitrogen fixation. These mechanisms are more critical in natural and agricultural conditions, where various combinations of legume and rhizobia can occur.

It is also possible that rhizobia have acquired specialized proteins, such as HrrP and DCA1, to help bacteria to cheat: these proteins induce the cessation of nitrogen fixation after colonization of the nodule and the release of the increased bacterial population from the nonfunctional nodule without performing the "hard work" of nitrogen reduction. Conversely, host legumes have evolved a sanction mechanism to reduce the fitness of cheating rhizobia (72). As we have shown here, APN1 could be the response of the host plants in the "arms race" to control bacteria and to ensure that rhizobia perform the task for which they are allowed into the plant cells.

Understanding the strategies used by different legume and rhizobial species to select the favorable symbiotic partner in their natural habitat is extremely important to control and maximize the symbiotic performance. Our work clarified a novel aspect of the strategy of legumes to optimize symbiotic nitrogen fixation activity with a specific rhizobial strain.

Materials and Methods

Plant and microbial materials, plasmid constructions, nodulation assay, competition assay, mutant library construction, recombinant and secreted protein preparation, protease assay, measurement of free asparagine and glutamine contents, hairy root transformation, RNA-seq and real time RT-PCR, and computer analysis are described in *SI Appendix, Materials and Methods*.

Data Availability. The data that support the findings of this study are available in *SI Appendix* and Gene Expression Omnibus under the accession number GSE129778.

ACKNOWLEDGMENTS. We thank Daniel J. Gage (University of Connecticut), Shin Okazaki (Tokyo University of Agriculture and Technology), and Tsuneo Hakoyama (RIKEN) for kindly giving us the plasmids pDG77, pFAJpcycA, and pLb3-GW-tLb3, respectively. We also thank Hiroshi Ono (National Agriculture and Food Research Organization) for his technical advice on free amino acid measurement in plants. This work was funded by Japan Society for the Promotion of Science KAKENHI grants to Y.S. (nos. JP25712006 and JP18K05381).

1. H. Kouchi *et al*., How many peas in a pod? Legume genes responsible for mutualistic symbioses underground. *Plant Cell Physiol.* **51**, 1381–1397 (2010).
2. H. Kouchi, *Symbiotic Nitrogen Fixation, Plant Metabolism and Biotechnology*, H. Ashihara, A. Crozier, A. Komamine, Eds. (John Wiley & Sons, Ltd., Hoboken, NJ, 2011).
3. G. E. Oldroyd, Speak, friend, and enter: Signalling systems that promote beneficial symbiotic associations in plants. *Nat. Rev. Microbiol.* **11**, 252–263 (2013).
4. E. B. Madsen *et al*., A receptor kinase gene of the LysM type is involved in legume perception of rhizobial signals. *Nature* **425**, 637–640 (2003).
5. S. Radutoiu *et al*., Plant recognition of symbiotic bacteria requires two LysM receptor-like kinases. *Nature* **425**, 585–592 (2003).
6. J. Lévy *et al*., A putative Ca^{2+} and calmodulin-dependent protein kinase required for bacterial and fungal symbioses. *Science* **303**, 1361–1364 (2004).
7. L. Tirichine *et al*., Deregulation of a Ca^{2+}/calmodulin-dependent kinase leads to spontaneous nodule development. *Nature* **441**, 1153–1156 (2006).
8. E. Messinese *et al*., A novel nuclear protein interacts with the symbiotic DMI3 calcium- and calmodulin-dependent protein kinase of *Medicago truncatula*. *Mol. Plant Microbe Interact.* **20**, 912–921 (2007).
9. K. Yano *et al*., CYCLOPS, a mediator of symbiotic intracellular accommodation. *Proc. Natl. Acad. Sci. U.S.A.* **105**, 20540–20545 (2008).
10. L. Schauser, A. Roussis, J. Stiller, J. Stougaard, A plant regulator controlling development of symbiotic root nodules. *Nature* **402**, 191–195 (1999).
11. L. Krusell *et al*., The sulfate transporter SST1 is crucial for symbiotic nitrogen fixation in Lotus japonicus root nodules. *Plant Cell* **17**, 1625–1636 (2005).
12. T. Hakoyama *et al*., Host plant genome overcomes the lack of a bacterial gene for symbiotic nitrogen fixation. *Nature* **462**, 514–517 (2009).
13. T. Hakoyama *et al*., The SNARE protein SYP71 expressed in vascular tissues is involved in symbiotic nitrogen fixation in *Lotus japonicus* nodules. *Plant Physiol.* **160**, 897–905 (2012).
14. T. Hakoyama *et al*., The integral membrane protein SEN1 is required for symbiotic nitrogen fixation in *Lotus japonicus* nodules. *Plant Cell Physiol.* **53**, 225–236 (2012).
15. H. Kumagai *et al*., A novel ankyrin-repeat membrane protein, IGN1, is required for persistence of nitrogen-fixing symbiosis in root nodules of *Lotus japonicus*. *Plant Physiol.* **143**, 1293–1305 (2007).
16. D. Wang *et al*., A nodule-specific protein secretory pathway required for nitrogen-fixing symbiosis. *Science* **327**, 1126–1129 (2010).
17. M. Bourcy *et al*., *Medicago truncatula* DNF2 is a PI-PLC-XD-containing protein required for bacteroid persistence and prevention of nodule early senescence and defense-like reactions. *New Phytol.* **197**, 1250–1261 (2013).
18. P. Mergaert *et al*., A novel family in *Medicago truncatula* consisting of more than 300 nodule-specific genes coding for small, secreted polypeptides with conserved cysteine motifs. *Plant Physiol.* **132**, 161–173 (2003).
19. B. Horváth *et al*., Loss of the nodule-specific cysteine rich peptide, NCR169, abolishes symbiotic nitrogen fixation in the *Medicago truncatula dnf7* mutant. *Proc. Natl. Acad. Sci. U.S.A.* **112**, 15232–15237 (2015).
20. M. Kim *et al*., An antimicrobial peptide essential for bacterial survival in the nitrogen-fixing symbiosis. *Proc. Natl. Acad. Sci. U.S.A.* **112**, 15238–15243 (2015).
21. M. K. Udvardi, D. A. Day, Metabolite transport across symbiotic membranes of legume nodules. *Annu. Rev. Plant Physiol. Plant Mol. Biol.* **48**, 493–523 (1997).
22. B. N. Kaiser *et al*., Characterization of an ammonium transport protein from the peribacteroid membrane of soybean nodules. *Science* **281**, 1202–1206 (1998).
23. K. Takanashi *et al*., LjMATE1: A citrate transporter responsible for iron supply to the nodule infection zone of Lotus japonicus. *Plant Cell Physiol.* **54**, 585–594 (2013).
24. I. S. Kryvoruchko *et al*., An iron-activated citrate transporter, MtMATE67, is required for symbiotic nitrogen fixation. *Plant Physiol.* **176**, 2315–2329 (2018).
25. P. Mergaert *et al*., Eukaryotic control on bacterial cell cycle and differentiation in the Rhizobium-legume symbiosis. *Proc. Natl. Acad. Sci. U.S.A.* **103**, 5230–5235 (2006).
26. W. Van de Velde *et al*., Plant peptides govern terminal differentiation of bacteria in symbiosis. *Science* **327**, 1122–1126 (2010).
27. P. Czernic *et al*., Convergent evolution of endosymbiont differentiation in dalbergioid and inverted repeat-lacking clade legumes mediated by nodule-specific cysteine-rich peptides. *Plant Physiol.* **169**, 1254–1265 (2015).
28. F. Lamouche, N. Bonadé-Bottino, P. Mergaert, B. Alunni, Symbiotic efficiency of spherical and elongated bacteroids in the *Aeschynomene-Bradyrhizobium* symbiosis. *Front. Plant Sci.* **10**, 377 (2019).
29. Q. Wang *et al*., Host-secreted antimicrobial peptide enforces symbiotic selectivity in *Medicago truncatula*. *Proc. Natl. Acad. Sci. U.S.A.* **114**, 6854–6859 (2017).
30. Q. Wang *et al*., Nodule-specific cysteine-rich peptides negatively regulate nitrogen-fixing symbiosis in a strain-specific manner in *Medicago truncatula*. *Mol. Plant Microbe Interact.* **31**, 240–248 (2018).
31. S. Yang *et al*., Microsymbiont discrimination mediated by a host-secreted peptide in *Medicago truncatula*. *Proc. Natl. Acad. Sci. U.S.A.* **114**, 6848–6853 (2017).
32. H. Yamaya-Ito *et al*., Loss-of-function of ASPARTIC PEPTIDASE NODULE-INDUCED 1 (APN1) in *Lotus japonicus* restricts efficient nitrogen-fixing symbiosis with specific *Mesorhizobium loti* strains. *Plant J.* **93**, 5–16 (2018).
33. M. Kawaguchi *et al*., Root, root hair, and symbiotic mutants of the model legume *Lotus japonicus*. *Mol. Plant Microbe Interact.* **15**, 17–26 (2002).
34. Y. Shimoda, H. Hirakawa, S. Sato, K. Saeki, M. Hayashi, Whole genome sequence of the nitrogen-fixing symbiotic rhizobia *Mesorhizobium loti* strain TONO. *Genome Announc.* **4**, e01016-16 (2016).
35. T. Kaneko *et al*., Complete genome structure of the nitrogen-fixing symbiotic bacterium *Mesorhizobium loti*. *DNA Res.* **7**, 331–338 (2000).
36. F. Berrabah *et al*., A nonRD receptor-like kinase prevents nodule early senescence and defense-like reactions during symbiosis. *New Phytol.* **203**, 1305–1314 (2014).
37. Y. Shimoda *et al*., Construction of signature-tagged mutant library in *Mesorhizobium loti* as a powerful tool for functional genomics. *DNA Res.* **15**, 297–308 (2008).
38. M. Junker *et al*., Pertactin beta-helix folding mechanism suggests common themes for the secretion and folding of autotransporter proteins. *Proc. Natl. Acad. Sci. U.S.A.* **103**, 4918–4923 (2006).
39. X. Yuan *et al*., Molecular basis for the folding of β-helical autotransporter passenger domains. *Nat. Commun.* **9**, 1395 (2018).
40. S. Kelly *et al*., Genome sequence of the Lotus spp. microsymbiont *Mesorhizobium loti* strain R7A. *Stand. Genomic Sci.* **9**, 6 (2014).
41. B. van den Berg, Crystal structure of a full-length autotransporter. *J. Mol. Biol.* **396**, 627–633 (2010).
42. Y. Zhang, I-TASSER server for protein 3D structure prediction. *BMC Bioinformatics* **9**, 40 (2008).
43. I. R. Henderson, F. Navarro-Garcia, M. Desvaux, R. C. Fernandez, D. Ala'Aldeen, Type V protein secretion pathway: The autotransporter story. *Microbiol. Mol. Biol. Rev.* **68**, 692–744 (2004).
44. N. R. Movva, K. Nakamura, M. Inouye, Amino acid sequence of the signal peptide of ompA protein, a major outer membrane protein of Escherichia coli. *J. Biol. Chem.* **255**, 27–29 (1980).
45. D. J. Gage, Analysis of infection thread development using Gfp- and DsRed-expressing *Sinorhizobium meliloti*. *J. Bacteriol.* **184**, 7042–7046 (2002).
46. Y. Xia *et al*., An extracellular aspartic protease functions in *Arabidopsis* disease resistance signaling. *EMBO J.* **23**, 980–988 (2004).
47. J. E. Olivares *et al*., Nodulin 41, a novel late nodulin of common bean with peptidase activity. *BMC Plant Biol.* **11**, 134 (2011).
48. M. Ramalho-Santos *et al*., Identification and proteolytic processing of procardosin A. *Eur. J. Biochem.* **255**, 133–138 (1998).
49. K. N. Lohman, S. S. Gan, M. C. John, R. M. Amasino, Molecular analysis of natural leaf senescence in Arabidopsis thaliana. *Physiol. Plant.* **92**, 322–328 (1994).
50. J. C. Pérez Guerra *et al*., Comparison of developmental and stress-induced nodule senescence in Medicago truncatula. *Plant Physiol.* **152**, 1574–1584 (2010).
51. S. G. van Wyk, M. Du Plessis, C. A. Cullis, K. J. Kunert, B. J. Vorster, Cysteine protease and cystatin expression and activity during soybean nodule development and senescence. *BMC Plant Biol.* **14**, 294 (2014).
52. S. Sinharoy *et al*., The C2H2 transcription factor regulator of symbiosome differentiation represses transcription of the secretory pathway gene VAMP721a and promotes symbiosome development in *Medicago truncatula*. *Plant Cell* **25**, 3584–3601 (2013).
53. C. Wang *et al*., NODULES WITH ACTIVATED DEFENSE 1 is required for maintenance of rhizobial endosymbiosis in *Medicago truncatula*. *New Phytol.* **212**, 176–191 (2016).
54. B. E. Caldwell, Inheritance of a strain specific-ineffective nodulation in soybeans. *Crop Sci.* **6**, 427–428 (1966).
55. T. A. Lie, Gene centers, a source for genetic variants in symbiotic nitrogen fixation: Host induced ineffectivity in *Pisum sativum* ecotype *fulvum*. *Plant Soil* **61**, 125–134 (1981).
56. G. Duc, J. Picard, Note on the presence of the Sym-1 gene in *Vicia faba* hampering the symbiosis with *Rhizobium leguminosarum*. *Euphytica* **35**, 61–64 (1986).
57. N. Dautin, H. D. Bernstein, Protein secretion in gram-negative bacteria via the autotransporter pathway. *Annu. Rev. Microbiol.* **61**, 89–112 (2007).
58. J. C. Leo, I. Grin, D. Linke, Type V secretion: Mechanism(s) of autotransport through the bacterial outer membrane. *Philos. Trans. R. Soc. Lond. B Biol. Sci.* **367**, 1088–1101 (2012).
59. T. Suzuki *et al*., An outer membrane autotransporter, AoaA, of *Azorhizobium caulinodans* is required for sustaining high N2-fixing activity of stem nodules. *FEMS Microbiol. Lett.* **285**, 16–24 (2008).
60. C. I. Pislariu *et al*., The nodule-specific PLAT domain protein NPD1 is required for nitrogen-fixing symbiosis. *Plant Physiol.* **180**, 1480–1497 (2019).
61. F. Berrabah, P. Ratet, B. Gourion, Multiple steps control immunity during the intracellular accommodation of rhizobia. *J. Exp. Bot.* **66**, 1977–1985 (2015).
62. I. Hara-Nishimura, N. Hatsugai, S. Nakaune, M. Kuroyanagi, M. Nishimura, Vacuolar processing enzyme: An executor of plant cell death. *Curr. Opin. Plant Biol.* **8**, 404–408 (2005).
63. O. Pierre *et al*., Involvement of papain and legumain proteinase in the senescence process of *Medicago truncatula* nodules. *New Phytol.* **202**, 849–863 (2014).
64. N. Suganuma *et al*., cDNA macroarray analysis of gene expression in ineffective nodules induced on the *Lotus japonicus* sen1 mutant. *Mol. Plant Microbe Interact.* **17**, 1223–1233 (2004).
65. C. I. Pislariu *et al*., A *Medicago truncatula* tobacco retrotransposon insertion mutant collection with defects in nodule development and symbiotic nitrogen fixation. *Plant Physiol.* **159**, 1686–1699 (2012).
66. V. C. Clarke *et al*., Proteomic analysis of the soybean symbiosome identifies new symbiotic proteins. *Mol. Cell. Proteomics* **14**, 1301–1322 (2015).
67. O. Pierre *et al*., Peribacteroid space acidification: A marker of mature bacteroid functioning in *Medicago truncatula* nodules. *Plant Cell Environ.* **36**, 2059–2070 (2013).
68. M. S. Nelson, M. J. Sadowsky, Secretion systems and signal exchange between nitrogen-fixing rhizobia and legumes. *Front. Plant Sci.* **6**, 491 (2015).
69. S. Okazaki, S. Zehner, J. Hempel, K. Lang, M. Göttfert, Genetic organization and functional analysis of the type III secretion system of *Bradyrhizobium elkanii*. *FEMS Microbiol. Lett.* **295**, 88–95 (2009).
70. S. Yang, F. Tang, M. Gao, H. B. Krishnan, H. Zhu, R gene-controlled host specificity in the legume-rhizobia symbiosis. *Proc. Natl. Acad. Sci. U.S.A.* **107**, 18735–18740 (2010).
71. P. A. Price *et al*., Rhizobial peptidase HrrP cleaves host-encoded signaling peptides and mediates symbiotic compatibility. *Proc. Natl. Acad. Sci. U.S.A.* **112**, 15244–15249 (2015).
72. J. L. Sachs, K. W. Quides, C. E. Wendlandt, Legumes versus rhizobia: A model for ongoing conflict in symbiosis. *New Phytol.* **219**, 1199–1206 (2018).
73. T. L. Bailey, C. Elkan, Fitting a mixture model by expectation maximization to discover motifs in biopolymers. *Proc. Int. Conf. Intell. Syst. Mol. Biol.* **2**, 28–36 (1994).
74. L. J. McGuffin, K. Bryson, D. T. Jones, The PSIPRED protein structure prediction server. *Bioinformatics* **16**, 404–405 (2000).